Understanding hydrogen and nitrogen doping on active defects in amorphous In-Ga-Zn-O thin film transistors

Guoli Li, Ablat Abliz, Lei Xu, Nicolas André, Xingqiang Liu, Yun Zeng, Denis Flandre, and Lei Liao

Citation: Appl. Phys. Lett. **112**, 253504 (2018); doi: 10.1063/1.5032169
View online: https://doi.org/10.1063/1.5032169
View Table of Contents: http://aip.scitation.org/toc/apl/112/25
Published by the American Institute of Physics

Understanding hydrogen and nitrogen doping on active defects in amorphous In-Ga-Zn-O thin film transistors

Guoli Li,[1] Ablat Abliz,[2] Lei Xu,[1] Nicolas André,[3] Xingqiang Liu,[1] Yun Zeng,[1,a)] Denis Flandre,[1,3] and Lei Liao[1,4,a)]
[1]*Key Laboratory for Micro-/Nano-Optoelectronic Devices of Ministry of Education, School of Physics and Electronics, Hunan University, Changsha 410082, China*
[2]*School of Physics Science and Technology, Xinjiang University, Urumqi 830046, China*
[3]*The ICTEAM Institute, Université catholique de Louvain, Louvain-la-Neuve B-1348, Belgium*
[4]*School of Physics and Technology, Wuhan University, Wuhan 430072, China*

(Received 3 April 2018; accepted 5 June 2018; published online 20 June 2018)

This work analyses the physics of active trap states impacted by hydrogen (H) and nitrogen (N) dopings in amorphous In-Ga-Zn-O (a-IGZO) thin-film transistors (TFTs) and investigates their effects on the device performances under back-gate biasing. Based on numerical simulation and interpretation of the device transfer characteristics, it is concluded that the interface and bulk tail states, as well as the 2+ charge states (i.e., acceptors V_O^{2+}) related to oxygen vacancy (V_O), are neutralized by the H/N dopants incorporation via an experimental plasma treatment. Moreover, the simulation reveals that an acceptor-like defect V_OH has been induced by the H doping, to support the observed additional degradation of device subthreshold slope. Superior stability of the optimized a-IGZO TFTs under a proper amount of H/N doping is demonstrated by the decreased density of V_O-related defects in simulation, where hole (V_O^0 donor) and electron trapping (O_i acceptor) occurs during the negative or positive bias stresses. This work benefit lies in an in-depth systematic understanding and exploration of the effects of the incorporation of the H and N dopants into the a-IGZO film for the TFTs improvement and optimization. *Published by AIP Publishing.*
https://doi.org/10.1063/1.5032169

Amorphous indium-gallium-zinc oxide (a-IGZO) has been widely used as an active channel layer of thin-film transistors (TFTs) for their applications in high-definition active matrix liquid crystal displays, due to its desirable electron mobility, high optical transparency, low process temperature, and mechanical flexibility.[1–3] However, traps and native point defects,[4] unavoidably existing in the IGZO channel and at the channel/insulator layer interfaces, lead to device instability problems, shift in threshold voltage (V_{TH}) as well as degradations in field-effect mobility (μ_{FE}), subthreshold slope (*SS*), and leakage and saturation currents.[5]

Dopants incorporation (e.g., phosphorus, nitrogen, hydrogen, and argon[6–9]) into the a-IGZO was widely explored with the aim of producing high-performance TFTs, by modulating the carrier concentration (N_e), improving the interface quality, and reducing the native point defect states, e.g., defects related to oxygen vacancies (V_O) in a-IGZO TFTs. Nitrogen (N) doping was performed *in-situ* during the IGZO film deposition to improve the device performance, with an optimized carrier mobility of 19.21 $cm^2\ V^{-1}\ s^{-1}$ and subthreshold swing of 0.26 V/decade in Ref. 8. N acts as an acceptor and serves as a defect binder, as the ionic radius of N is close to that of oxygen (O), to effectively substitute for O and reduce V_O in the IGZO film and lead to a decrease in carrier concentration.[10] Hydrogen (H) incorporation in an a-IGZO film was found to passivate native defects and increase the electron concentration,[11,12] as H can act as a shallow n-type donor, occupy interstitial positions (H_i) or V_O sites, and exhibit strong bonding with oxygen (O-H) during a H plasma treatment.[13] However, a large increase in the quantity of dopants incorporation into the samples may result in an increase in the oxygen vacancies as well as the dopants-related defects.[14] Excessive H or N doping could undesirably lead to large V_{TH} shift and degrade μ_{FE} of the a-IGZO TFTs.[15]

Despite intensive research on improving electrical performances of the a-IGZO TFTs by incorporating H and N dopants, with respect to experimental observations and theoretical analyses, device simulation and modeling have not been done yet to quantitatively clarify how the H and N dopings impact on each type of traps (i.e., the interface and bulk traps, the native point defects) in the a-IGZO and qualitatively interpret the trap influence on the device behavior thereafter.

In this work, the numerical device simulation of a-IGZO TFTs has been conducted in ATLAS/Silvaco.[16] Based on modeling of the TFT transfer characteristics, this paper focuses on the interpretation of the device *SS*, V_{TH}, and stability under different doping conditions (as obtained experimentally via a plasma treatment in Ref. 15), in order to identify each type of the active defects which are impacted by the H or N doping and affect the electrical device performances under back-gate bias sweep.

As the literature indicates, the plasma treatment has been demonstrated as an alternative and efficient technique among the reported approaches for the dopants incorporation[17–19] and the low-temperature processing.[10,20] Optimal device performances of the a-IGZO TFTs have been obtained with an improved *SS* of 0.21 V/decade, μ_{FE} of 45.3 $cm^2\ V^{-1}\ s^{-1}$, and enhanced device stability (i.e., a small shift of V_{TH}) under

a)Authors to whom correspondence should be addressed: yunzeng@hnu.edu.cn and liaolei@whu.edu.cn

negative and positive bias stresses of 3600 s at room temperature,[15] after the H_2 and N_2 plasma treatment with the power and pressure conditions set to 50 W and 6.0 Pa (for the H/N codoping), respectively, and the substrate temperature kept at 150 °C.

Figure 1(a) depicts a schematic of the a-IGZO TFT used for the following device simulation, onto which H_2 and N_2 plasma treatments were carried out in experiments, for the dopants incorporation into the 25 nm-thick (T_IGZO) IGZO film. Details of the fabrication process, device geometry, and measurements can be found in Ref. 15. On the basis of the interface and bulk traps, as well as native point defects primarily described in the a-IGZO material system,[4,20–22] Fig. 1(b) illustrates the types of the defect states in the IGZO film and at the IGZO/gate dielectric interface which are proposed and investigated in this work. E_C denotes the conduction band minimum and E_V the valence band maximum. In the IGZO film, the conduction band tail states consist of the acceptor-like tail state (g_{TA}) and the acceptor-like deep states (g_{DA}), and the valence band tail states consist of the donor-like tail states (g_{TD}) and the donor-like deep states (g_{DD}). At the IGZO/dielectric interface, acceptor-like ($D_{it(A)}$) and donor-like ($D_{it(D)}$) tail states are discussed.[23]

Several types of the native point defects mainly need to be considered, with a Gaussian distribution as depicted in Fig. 1(b). For the neutral (Vo^0), 1+ (Vo^+), and 2+ (Vo^{2+}) charge states related to Vo, we focus on discussion of the stable charge states, namely, Vo^0 and Vo^{2+} in the present work,

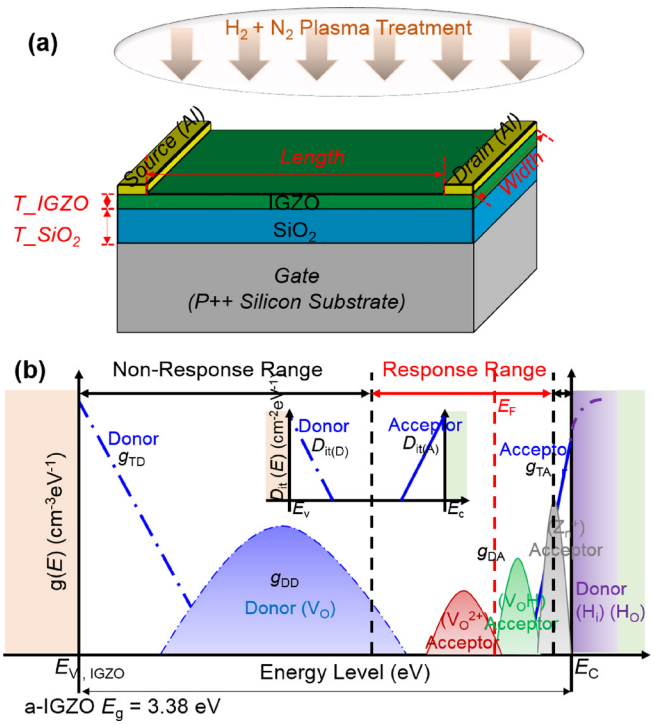

FIG. 1. (a) Schematic diagram of the a-IGZO TFT using silicon bottom gate; (b) Schematic illustration of trap states distribution in the bulk of the a-IGZO film, including the donor (g_{TD}) and acceptor (g_{TA}) tail states, and the donor (g_{DD}) and acceptor (g_{DA}) point states. The inset depicts the interface donor ($D_{it(D)}$) and acceptor ($D_{it(A)}$) tail states of the a-IGZO. The response range indicates the donor (acceptor) states levels which lie above (below) E_F under a back-gate bias sweep and thus electrically respond to the bias change, whereas the non-response range represents the states kept neutral under the back-gate bias sweep.

where the Vo^+ is unstable for any position of E_F.[4] Vo^0 defect is known to act as deep donor, $g_{DD}(Vo^0)$, with energy level at approximately 1.0–1.5 eV above the E_V.[23] Electron capture takes place for the Vo^{2+}, $g_{DA}(Vo^{2+})$, which lies at ~2.85 eV above the E_V, as an acceptor.[24] Moreover, in the n-type IGZO sample, zinc vacancies (V_{zn}) also easily form as deep acceptors with transition level of 0.18 eV,[4] $g_{DA}(V_{zn})$. To focus on the Vo-related defects which are impacted by the plasma treatment and therefore electrically respond under stability characterization as will be discussed in the last paragraph, $g_{DA}(V_{zn})$ is kept constant in this research. The V_OH, H_O, and H_i defects in Fig. 1(b) related to the plasma treatment will be discussed later.

Electrons can flow into and out of these donor and acceptor states depending on the position of the Fermi level, which means that the charge state of the defects (i.e., donor and acceptor) changes while the position of the Fermi level is altered. The donors become positively charged if the Fermi level is below it and is neutral when the trap is occupied (i.e., the Fermi level is above it). The acceptor is neutral if the Fermi level is below the defect state and become negatively charged if the Fermi level is above it.

To analyze the impact of the different H_2, N_2, and H_2/N_2 plasma treatments on defects and therefore on the device performances, transfer characteristics (drain current versus gate voltage, i.e., I_{DS}–V_{GS}) of the a-IGZO TFT are simulated in ATLAS/Silvaco,[16,25] using the traps described above and with the uniform distribution of the bulk traps (i.e., native point defects) inside the a-IGZO film. In the simulation set-up, volume carrier mobility is initially set as 45 $cm^2\ V^{-1}\ s^{-1}$, consistent with the experimental value extracted in the device after H_2 and N_2 plasma treatment of 200-s duration ("H/N:200 s").[15] Volume carrier lifetime is 1 ns. Bandgap of the IGZO material is 3.38 eV, with affinity of 4.16 eV.[5] An "intrinsic" electron density (with corresponding $E_F = 1.09$ eV) is set into the a-IGZO film, due to "unintentional" doping condition induced by the amorphous structure and the states related to the V_O.[23] The source and drain are implemented as Schottky contacts, while P^+ polysilicon is specified as the back-gate contact material.

A back-gate bias (V_{GS}) sweep from −20 V to +20 V is applied to the P^+ silicon substrate, to shift the Fermi level (E_F) in the bandgap. The E_F in an ideal a-IGZO TFT without considering traps can be shifted from $E_F - E_V = 0.174$ (0.244) eV to $E_C - E_F = 0.145$ (0.296) eV at the back (front) surface of the 25 nm-thick a-IGZO film. However, the E_F is also relevant to the trap conditions, in practice, due to the pinning effect.[26] The trap states (i.e., donors and acceptors) in the IGZO film and at the IGZO/insulator interface electrically affect the device performance (transfer characteristics, *SS* and V_{TH}), depending on the E_F, whereas the donor states always below the E_F and the acceptor states always above the E_F are electrically inactive under the gate biasing as depicted in Fig. 1(b) by the response/non-response ranges.

Figure 2(a) presents the simulation results of the I_{DS}-V_{GS} curves, after calibrating the defect model parameters to be consistent with the experimental observations of Ref. 15, at drain bias $V_{DS} = 1.0$ V, for the a-IGZO TFTs under different doping conditions, i.e., no plasma treatment (undoped), H_2 plasma treatment of 100-s time ("H:100 s"), N_2 plasma

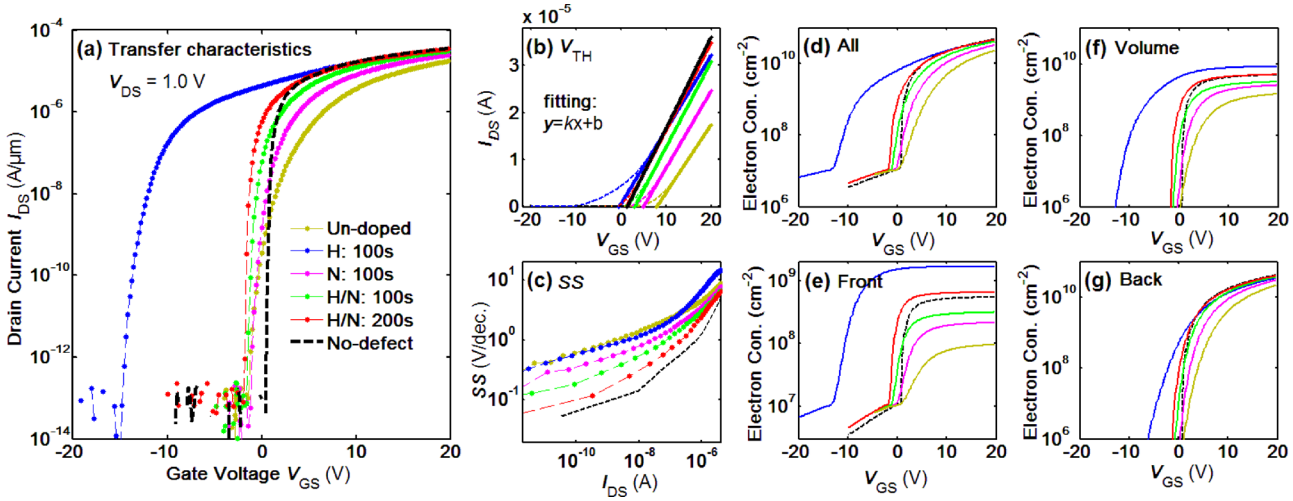

FIG. 2. (a) Simulated transfer characteristics [I_{DS} *(per μm of device width) vs* V_{GS}] at $V_{DS} = 1.0$ V for a-IGZO TFTs of Fig. 1, with defect model parameters given in Table I, as calibrated on experimental curves of Ref. 15 obtained after different doping conditions: undoped, H:100 s, N:100 s, H/N:100 s, H/N:200 s, and No-defect. (b) Threshold voltage (V_{TH}) extraction in the linear regime. (c) Subthreshold slope (*SS*) as a function of drain current I_{DS}; integrated electron concentration as a function of V_{GS}, (d) through the whole channel, (e) around the front interface, (f) in the volume film, and (g) around the back interface in the a-IGZO TFTs under different doping conditions.

treatment of 100-s time ("N:100 s"), H_2 and N_2 plasma treatment of 100-s time ("H/N:100 s") and of 200-s time ("H/N:200 s"), and an ideal case (No-defect) as a reference.

Compared to the undoped a-IGZO TFT, with open voltage of the subthreshold region (defined at a current of 10^{-13} A/μm) $V_0 = -1.2$ V in Fig. 2(a), the V_0 in the a-IGZO with "H:100 s" is −14.54 V, indicating that positive charges are directly introduced by the H dopants, whereas the V_0 in the a-IGZO with "N:100 s" is increased to be −1.0 V indicating a slight decrease in positive charges caused by the N doping.

The optimal device performance is obtained in the a-IGZO TFT with "H/N:200 s," with the highest μ_{FE} observed in experiments as well as optimized V_{TH} and *SS* and shown in Figs. 2(b) and 2(c) to be close to the ideal case where no defect is included (i.e., the black dashed curve). The V_{TH} of Fig. 2(b) is extracted based on a linear fitting in the I_{DS}-V_{GS} curves, as $V_{DS} = 1.0$ V is small and the a-IGZO TFTs work in the linear regime. The a-IGZO TFT with "H/N:200 s" shows a V_{TH} of 1.2 V close to the value of 1.3 V obtained for the ideal a-IGZO TFT. The *SS* of Fig. 2(c) is extracted in the drain current I_{DS} range of 10^{-12}–10^{-5} A. The optimized *SS* of 0.24 V/decade is obtained in the a-IGZO TFT with "H/N:200 s," close to the value of the ideal case (No-defect). These observations imply that traps can be neutralized by a proper amount of H/N co-doping. It is indeed well known that the V_{TH} and *SS* of the TFTs are related to the interface trap density (D_{it}) and the number of deep states, such that *SS* can be described as[27]

$$SS = \frac{qk_BT(N_{bulk}t_{ch} + D_{it})}{C_i log(e)}, \quad (1)$$

where q is the electron charge, k_B is the Boltzmann's constant, T is the absolute temperature, C_i is the capacitance of the gate dielectric, and t_{ch} is the active channel layer thickness. N_{bulk} is the semiconductor bulk traps density.

Furthermore, compared to the *SS* of the undoped case, the decrease in *SS* in the a-IGZO TFT with "N:100 s" indicates a decrease in traps density (D_{it} or N_{bulk}) by about a factor of 2 due to the N doping, whereas the high *SS* and its increase at $I_{DS} > 10^{-6}$ A observed in the a-IGZO TFT with "H:100 s" in Fig. 2(c) further indicate significant traps introduction by the H doping.

Integrated electron concentration through the whole channel, around the front interface, in the volume film, and around the back interface of the a-IGZO TFTs, is separately depicted in Figs. 2(d)–2(g) to illustrate the different components of device output drain current. The high level of integrated electron concentration in Fig. 2(g) while $V_{GS} > V_{TH}$ confirms that the device drain current is mainly contributed by the back surface as was discussed in Ref. 15 and thus related to the interface traps states. Moreover, with the uniform distribution of the native point defects, the simulated electron concentration (cm^{-3}) from the top to bottom side of the a-IGZO film (i.e., with the depth from 1 to 25 nm) has further validated that the TFT device characteristics are mainly affected by the back surface region (depth around 20–25 nm) of the a-IGZO film whatever the distribution of the native point defects. At $V_{GS} = 0$ V, the high integrated electron concentration in Figs. 2(e) and 2(f) indicates the high conductivity and external carrier concentration N_e introduced by the H doping. A further demonstration is done, with the conduction band energy level offsets ΔE_{CB} ($=E_C - E_F$) extracted in the a-IGZO TFTs left undoped and treated with "H:100 s" at $V_{GS} = 0.0$ V, being 0.525 eV and 0.307 eV separately.

To clarify how each type of defects changes under different doping and further identify its effect on device performances (i.e., *SS*, V_{TH}), Table I lists and summarizes the active defects that are electrically active in the device simulations of Fig. 2 and the traps description in Fig. 1(b).

After H doping, H passivates the interfacial trap states at the a-IGZO/dielectric interface,[9,14] which affect the *SS* as the device turns from OFF to ON state. Related to the role of H as a shallow donor, an increase in the Vo^0 and Vo^{2+} is stated, where the Vo related to the oxygen deficient bonding of the a-IGZO film increase with the H incorporation. A degradation of *SS* in the a-IGZO TFT with "H:100s" observed in

TABLE I. Densities of electrically active trap states fitted after different plasma treatment conditions.

States	Undoped	H:100 s	N:100 s	H/N:100 s	H/N:200 s
$D_{it(D)}$ ($cm^{-2}\,eV^{-1}$)	2×10^{13} *SS*–, V_{TH}–	↓1×10^{13}	↓1×10^{13}	↓0	0, Neutralized
$D_{it(A)}$ ($cm^{-2}\,eV^{-1}$)	2×10^{13} *SS*↑, V_{TH}→	↓1×10^{13}	↓1×10^{13}	↓0	0, Neutralized
g_{TD} ($cm^{-3}\,eV^{-1}$)	1×10^{20} *SS*–, V_{TH}–	1×10^{20}	↓5×10^{19}	↓5×10^{19}	0, Neutralized
g_{TA} ($cm^{-3}\,eV^{-1}$)	5×10^{19} *SS*↑, V_{TH}→	5×10^{19}	↓2.5×10^{19}	↓2.5×10^{19}	0, Neutralized
g_{DA} (V_{zn}) ($cm^{-3}\,eV^{-1}$)	1×10^{18} SS_2[b]↑,V_{TH}→	1×10^{18}	1×10^{18}	1×10^{18}	1×10^{18}
g_{DA} (V_O^{2+}) ($cm^{-3}\,eV^{-1}$)	1×10^{17} *SS*↑, V_{TH}→	↑3.2×10^{17}	↓5×10^{16}	↓0	0, Neutralized
g_{DD} (V_O^0)[a] ($cm^{-3}\,eV^{-1}$)	1.8×10^{17} *SS*–,V_{TH}←	↑2.0×10^{17}	↓1.5×10^{17}	↓1.5×10^{17}	↓1.5×10^{17}
g_{DD} (H_i) ($cm^{-3}\,eV^{-1}$)	…	↑2×10^{17} *SS*–, V_{TH}←	…	0, Neutralized	0, Neutralized
g_{DD} (H_O) ($cm^{-3}\,eV^{-1}$)	…	↑1×10^{18} *SS*–, V_{TH}←	…	2.5×10^{16}	5×10^{16}
g_{DA} (V_OH) ($cm^{-3}\,eV^{-1}$)	…	↑2×10^{17} SS_2↑, V_{TH}→	…	0, Neutralized	0, Neutralized

[a]$g_{DD}(V_O^0)$ is the equivalent density of the Vo^0 defects that are electrically responded under the gate biasing.
[b]SS_2 denotes the *SS* in the drain current 10^{-7}–10^{-5} A range.

Fig. 2(c) confirms the increase in $g_{DA}(Vo^{2+})$ in simulation. However, further degradation of *SS* at $I_{DS} > 10^{-6}$ A in this a-IGZO TFT cannot be explained by the Vo^{2+} defects. Based on our simulation understanding, it is found that an acceptor-like defect related to VoH complex has been created by H insertion into a Vo site (g_{DA}(VoH), at ~0.2 eV energy below the E_C), instead of probably behaving as a shallow donor state as in Ref. 13. The majority of H during the plasma treatment is bonded to O in the form of Ho.[11] The Ho defect acts as a donor and has a positive charge (1+) regardless of the E_F within the band gap. Interstitial hydrogen (H_i) is also predicted to act exclusively as a donor, i.e., always in the 1+ charge state.[27] These induced Ho and H_i defects are denoted by the purple bar and dashed curve in Fig. 1(b) and related to the large negative shift of V_{TH} and V_0 observed in the a-IGZO TFT with "H:100 s."

N is often considered as a promising p-type dopant and to serve as defect binder (i.e., facile substitution) due to its ionic radius close to that of O defects related to Vo. The tail states in the channel and at the channel/dielectric interface are reduced, which are confirmed by an improvement in V_{TH}, and *SS* of the a-IGZO TFTs with "N:100 s," as illustrated in Table I. However, a small degradation of V_{TH} instability and μ_{FE} in N-doped device was also observed,[15] which may be associated with the generation of N-related point defects.[27]

In the N-doped device, a small fraction of N substitutes for O and becomes an acceptor, i.e., No.[28] The N_O is stable in 1−charge state over most E_F energy range, thus is attracted by the positively charged H donors (Ho and H_i). Consequently, H atoms will tend to passivate the No acceptors (i.e., forming N-H bonds with N_O acceptors). That is, to say,, N_O^- and H_i^+ H_O^+ charged defects combine to form the neutral defect complexes, thereby compensating the N- and H- related defects, leading to the neutralization of H_i defects and the decrease in the high-density Ho defects in the H and N doping a-IGZO TFTs.

The enhanced *SS* and V_{TH} in the a-IGZO TFTs with "H/N:200 s," when compared to the ideal case of TFT (No-defect), indicate the neutralization of interfacial traps and V_O^{2+} point defects in the a-IGZO bulk and at the a-IGZO/SiO_2 interface, and the neutralization of the majority of the H-related donors by the H/N incorporation, as indicated in Table I. Moreover, the remaining shift of V_0 in this a-IGZO TFT in Fig. 2(a) indicates the existence of V_O^0 deep donor, which leads to the negative shift in the transfer characteristics and the possible existence of donor-like defect H_O related to H doping which also cause the shift without impact on device stability.

Based on the distribution of the trap states fitted in the a-IGZO TFT with "H/N:200 s," a quantitative investigation on the ΔV of transfer characteristics induced by negative bias stability (NBS) or positive bias stability (PBS) under a V_{GS} of ±20 V and stress duration of 3600 s is carried out. Experimental and simulated results are presented in Fig. 3(a). The NBS instability leads to a negative shift ($\Delta V = -2.6$ V) of the transfer characteristics, reproduced in the simulations by ionization of V_O^0 ($Vo^0 + 2h^+ \rightarrow Vo^{2+}$), i.e., V_O^0 acting as a hole trap[24] in Fig. 3(b). Under PBS, the oxygen interstitials (O_i) are demonstrated to be formed as deep acceptors, due to the weakly bonded oxygen ions. The created O_i in the

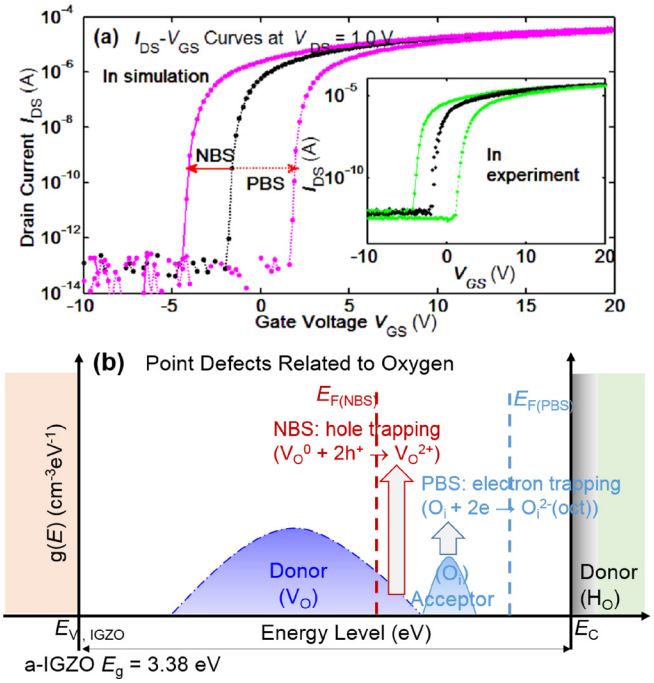

FIG. 3. (a) Transfer curves ($I_{DS} - V_{GS}$) at $V_{DS} = 1.0$ V of the a-IGZO TFTs "with H/N:200 s" after NBS ($V_{GS} = -20$ V) and PBS ($V_{GS} = +20$ V) with stress time of 3600 s. (b) Electrical response of oxygen-related defects under NBS and PBS.

octahedral configuration O_i(oct)[29] are electrically active and occupied by electrons (i.e., electron trapping) when the E_F under PBS is high, and thus negatively charged to form O_i^{2-}(oct), leading to a positive shift ($\Delta V = 3.4$ V) in the transfer curve. The optimized a-IGZO TFT has superior stability as compared to the undoped TFT under NBS and PBS (with a shift of $\pm\Delta V = \sim 10$ V), due to the decreased V_O-related defects.

To summarize, we simulated and presented detailed analyses of the active trap states which electrically impact the transfer characteristics of the a-IGZO TFTs under different H and N doping conditions as observed in previously reported experiments. To reproduce the large set of observations, completely and without ambiguity, 10 parameters have been implemented necessary and sufficient to model the defects and their impacts on the electrical characteristics as well as their clear dependencies on the dopants incorporation. The tail-distributed traps (i.e., g_{TA}, g_{TD}, $D_{it(A)}$, and $D_{it(D)}$) were reduced by the N doping (via N_2 plasma treatment of 100s), as well as the native point defects (i.e., Vo^0 and Vo^{2+}) related to Vo, with an improvement of the V_{TH}, and *SS* observed in the N-doped a-IGZO TFTs. The induced Ho and H_i defects were related to the large negative shift of V_{TH} observed in the a-IGZO TFT with the H dopants incorporation. Furthermore, an acceptor-like defect V_OH was found in simulation to be induced by the H dopants (via H_2 plasma treatment for 100 s) and to degrade the device *SS*. On the basis of experimental observations and theoretical investigations, the simulation indicates the neutralization of the interface and bulk tail states, and the 2+ charge states (i.e., acceptors V_O^{2+}) related to oxygen vacancy (V_O) in the a-IGZO film under a proper amount of H/N co-doping (via H_2 and N_2 plasma treatment for 200 s). Moreover, the reduction of V_O-related defects, responsible for the NBS and PBS, is shown to lead to improved device stability. This paper sheds light on using the simulations as a tool to fully investigate and interpret the impact of the H and N doping on the defects in the a-IGZO TFT and therefore optimize device fabrication and electrical performances.

This work was supported by the National Key Research and Development Program of China (2016YFB0401103), National Natural Science Funding of China (NSFC), under Grant Nos. 61574101, 11575132, 11604252 and 11574083, and the Technology Program (Major Project) of Changsha, under Grant No. kq1703001.

[1]X. G. Yu, T. J. Marks, and A. Facchetti, Nat. Mater. **15**, 383 (2016).
[2]T. Kamiya, K. Nomura, and H. Hosono, Sci. Technol. Adv. Mater. **11**, 044305 (2010).
[3]E. Fortunato, P. Barquinha, and R. Martins, Adv. Mater. **24**, 2945 (2012).
[4]A. Janotti and C. G. V. Walle, Phys. Rev. B **76**, 165202 (2007).
[5]A. Abliz, J. Wang, L. Xu, D. Wan, L. Liao, C. Ye, C. Liu, C. Jiang, H. Chen, and T. Guo, Appl. Phys. Lett. **108**, 213501 (2016).
[6]S. Parthiban and J. Y. Kwon, J. Mater. Res. **29**, 1585 (2014).
[7]R. Chen, W. Zhou, M. Zhang, M. Wong, and H. S. Kwok, IEEE Trans. Electron Devices **33**, 1150 (2012).
[8]P. T. Liu, C. H. Chang, C. S. Fuh, Y. T. Liao, and S. M. Sze, J. Disp. Technol. **12**, 1070 (2016).
[9]B. D. Ahn, H. S. Shin, H. J. Kim, J.-S. Park, and J. K. Jeong, Appl. Phys. Lett. **93**, 203506 (2008).
[10]J. Raja, K. Jang, N. Balaji, W. Choi, T. T. Trinh, and J. Yi, Appl. Phys. Lett. **102**, 083505 (2013).
[11]H. K. Noh, J. S. Park, and K. J. Chang, J. Appl. Phys. **113**, 063712 (2013).
[12]B. D. Ahn, J. S. Park, and K. B. Chung, Appl. Phys. Lett. **105**, 163505 (2014).
[13]M. Nakashima, M. Oota, N. Ishihara, Y. Nonaka, T. Hirohashi, M. Takahashi, S. Yamazaki, T. Ohonai, Y. Hosaka, and J. Koezuka, J. Appl. Phys. **116**, 213703 (2014).
[14]A. Song, H. Park, K. B. Chung, Y. S. Rim, K. S. Son, J. H. Lim, and H. Y. Chu, Appl. Phys. Lett. **111**, 243507 (2017).
[15]A. Abliz, Q. Gao, D. Wan, X. Liu, L. Xu, C. Liu, C. Jiang, X. Li, H. Chen, T. Guo, J. Li, and L. Liao, ACS Appl. Mater. Interfaces **9**, 10798 (2017).
[16]*Atlas User's Manual: Device Simulation Software* (Silvaco Inc., Santa Clara, USA, 2016).
[17]J. Zheng, R. Yang, L. Xie, J. Qu, Y. Liu, and X. Li, Adv. Mater. **22**, 1451 (2010).
[18]J. S. Kim, M. K. Joo, M. X. Piao, S. E. Ahn, Y. H. Choi, H. K. Jang, and G. T. Kim, J. Appl. Phys. **115**, 114503 (2014).
[19]H. Xie, Q. Wu, L. Xu, L. Zhang, G. Liu, and C. Dong, Appl. Surf. Sci. **387**, 237 (2016).
[20]Y. Kim, M. Bae, W. Kim, D. Kong, H. K. Jeong, H. Kim, S. Choi, D. M. Kim, and D. H. Kim, IEEE Trans. Electron Devices **59**, 2689 (2012).
[21]S. J. Lim, S. J. Kwon, and H. Kima, Appl. Phys. Lett. **91**, 183517 (2007).
[22]Y. Kim, S. Kim, W. Kim, M. Bae, H. K. Jeong, D. Kong, S. Choi, D. M. Kim, and D. H. Kim, IEEE Trans. Electron Devices **59**, 2699 (2012).
[23]J. T. Jang, J. Park, B. D. Ahn, D. M. Kim, S. Choi, H. Kim, and D. H. Kim, ACS Appl. Mater. Interfaces **7**, 15570 (2015).
[24]B. Ryu, H. Noh, E. Choi, and K. J. Chang, Appl. Phys. Lett. **97**, 022108 (2010).
[25]K. A. Stewart, V. Goulioukk, J. M. McGlone, and J. F. Wager, IEEE Trans. Electron Devices **64**, 4131 (2017).
[26]J. Zhu, R. Jhaveri, and J. C. S. Wooa, Appl. Phys. Lett. **96**, 193503 (2010).
[27]J. Raja, K. Jang, N. Balaji, and J. Yi, Semicond. Sci. Technol. **28**, 115010 (2013).
[28]X. Li, B. Keyes, S. Asher, S. B. Zhang, S. Wei, T. Coutts, S. Limpijumnong, and C. G. Van de Walle, Appl. Phys. Lett. **86**, 122107 (2005).
[29]X. Zhou, Y. Shao, L. Zhang, H. Lu, H. He, D. Han, Y. Wang, and S. Zhang, IEEE Electron Device Lett. **38**, 1252 (2017).